Electronic Supplementary Material (ESI) for Physical Chemistry Chemical Physics.

Supplementary Information

Water vapor effect on the physico-geometrical reaction pathway and kinetics of the multistep thermal dehydration of calcium chloride dihydrate

Kazuki Kato, Mito Hotta, and Nobuyoshi Koga*

Department of Science Education, Division of Educational Sciences, Graduate School of Humanities and Social Sciences, Hiroshima University, 1-1-1 Kagamiyama, Higashi-Hiroshima 739-8524, Japan

Contents

* Corresponding author. E-mail: nkoga@hiroshima-u.ac.jp

S1. Water vapor effect on the reaction pathway

Weibull function

$$F(t) = a_0 \left(\frac{a_3 - 1}{a_3}\right)^{\frac{1-a_3}{a_3}} \left\{\frac{t - a_1}{a_2} + \left(\frac{a_3 - 1}{a_3}\right)^{\frac{1}{a_3}}\right\}^{a_3 - 1} \exp\left[-\left\{\frac{t - a_1}{a_2} + \left(\frac{a_3 - 1}{a_3}\right)^{\frac{1}{a_3}}\right\}^{a_3} + \frac{a_3 - 1}{a_3}\right] \qquad \text{(S1)}$$

where a_0 is the amplitude, a_1 is the center, a_2 is the width, and a_3 is the shape parameters.

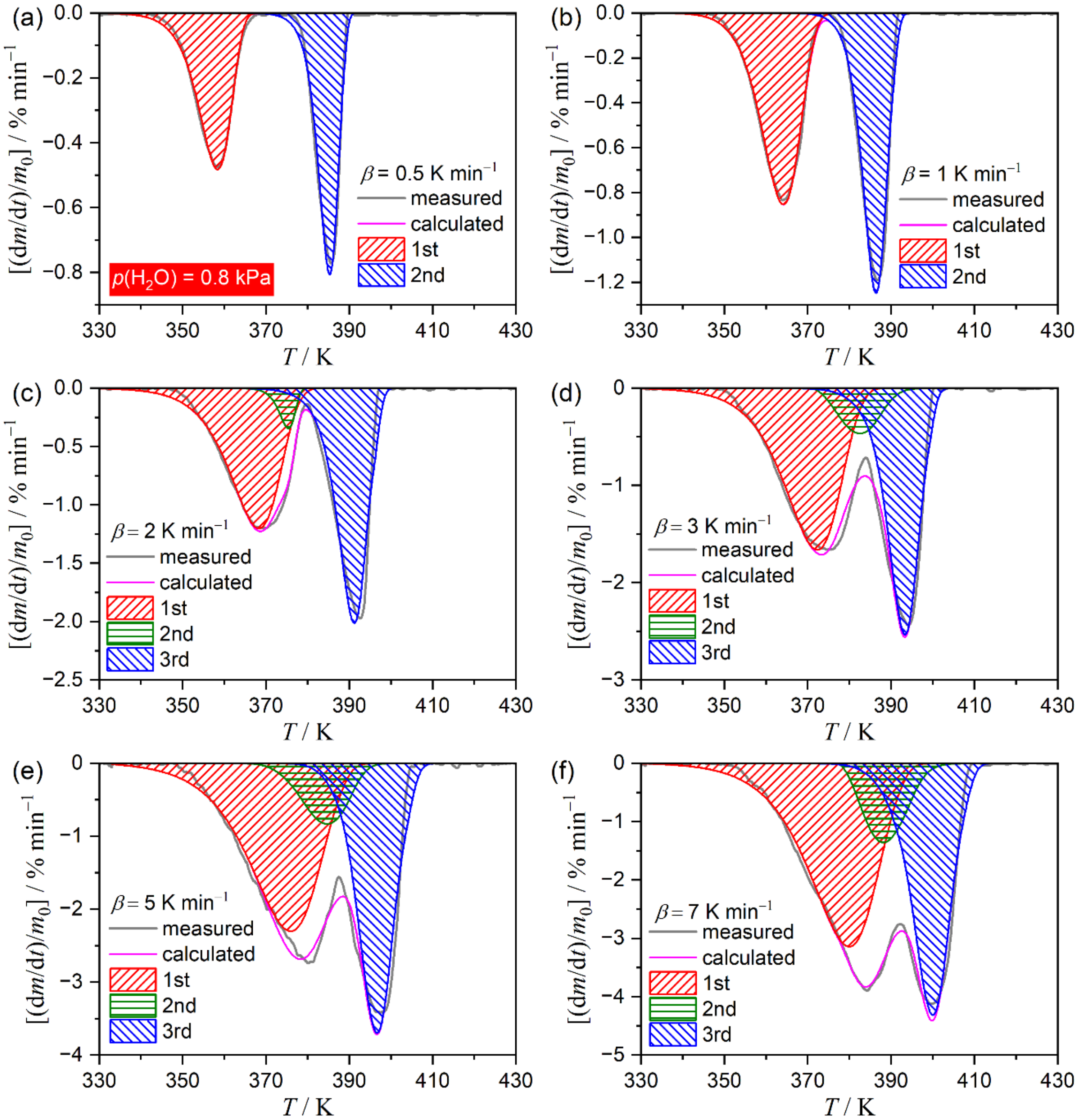

Figure S1. MDA results for the thermal dehydration process of CC-DH (m_0 = 3.01 ± 0.04 mg) to form CC-AH under linear nonisothermal conditions at various β values in a stream of wet N_2 with $p(H_2O)$ = 0.8 kPa.

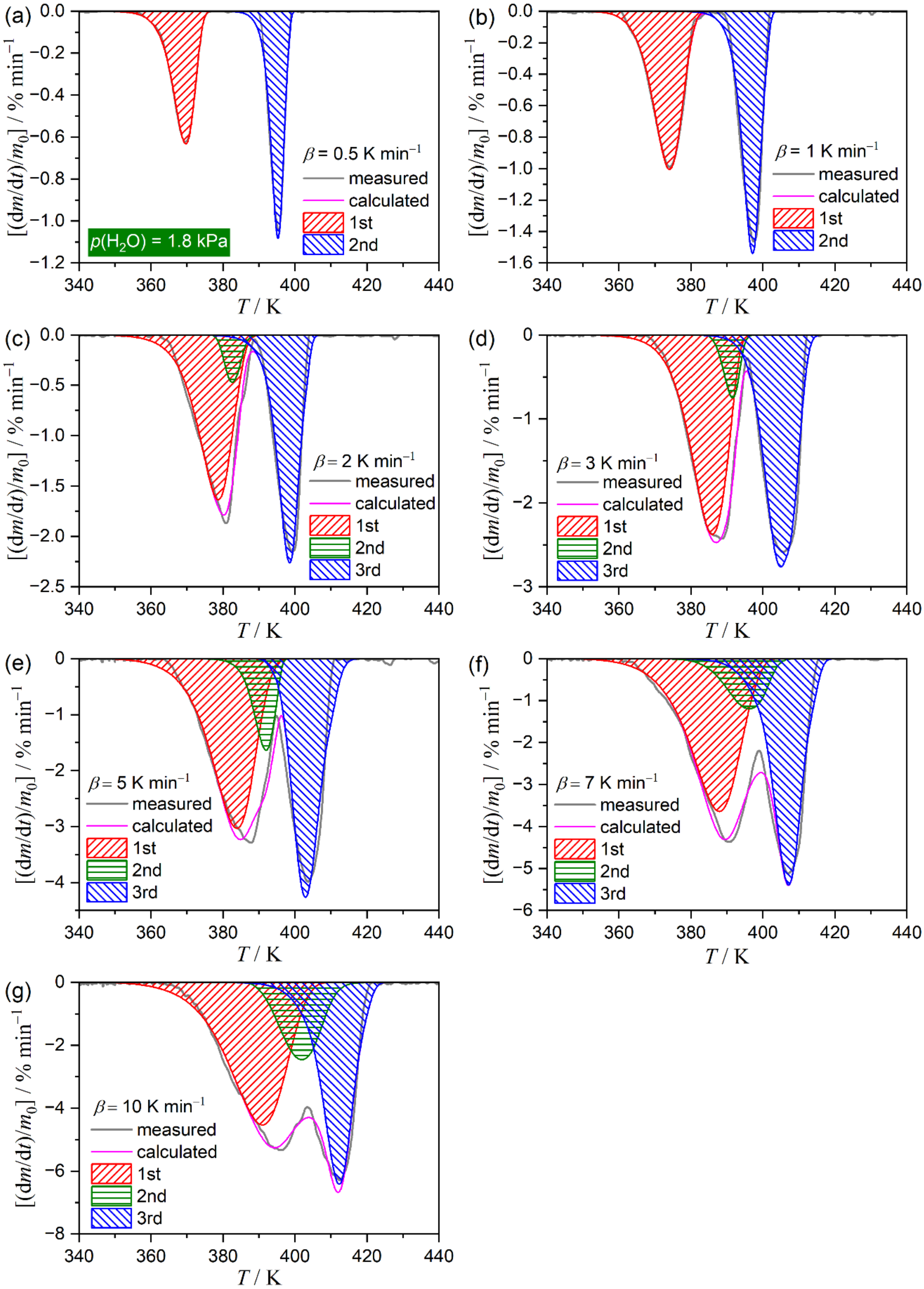

Figure S2. MDA results for the thermal dehydration process of CC-DH (m_0 = 3.02 ± 0.06 mg) to form CC-AH under linear nonisothermal conditions at various β values in a stream of wet N_2 with $p(H_2O)$ = 1.8 kPa.

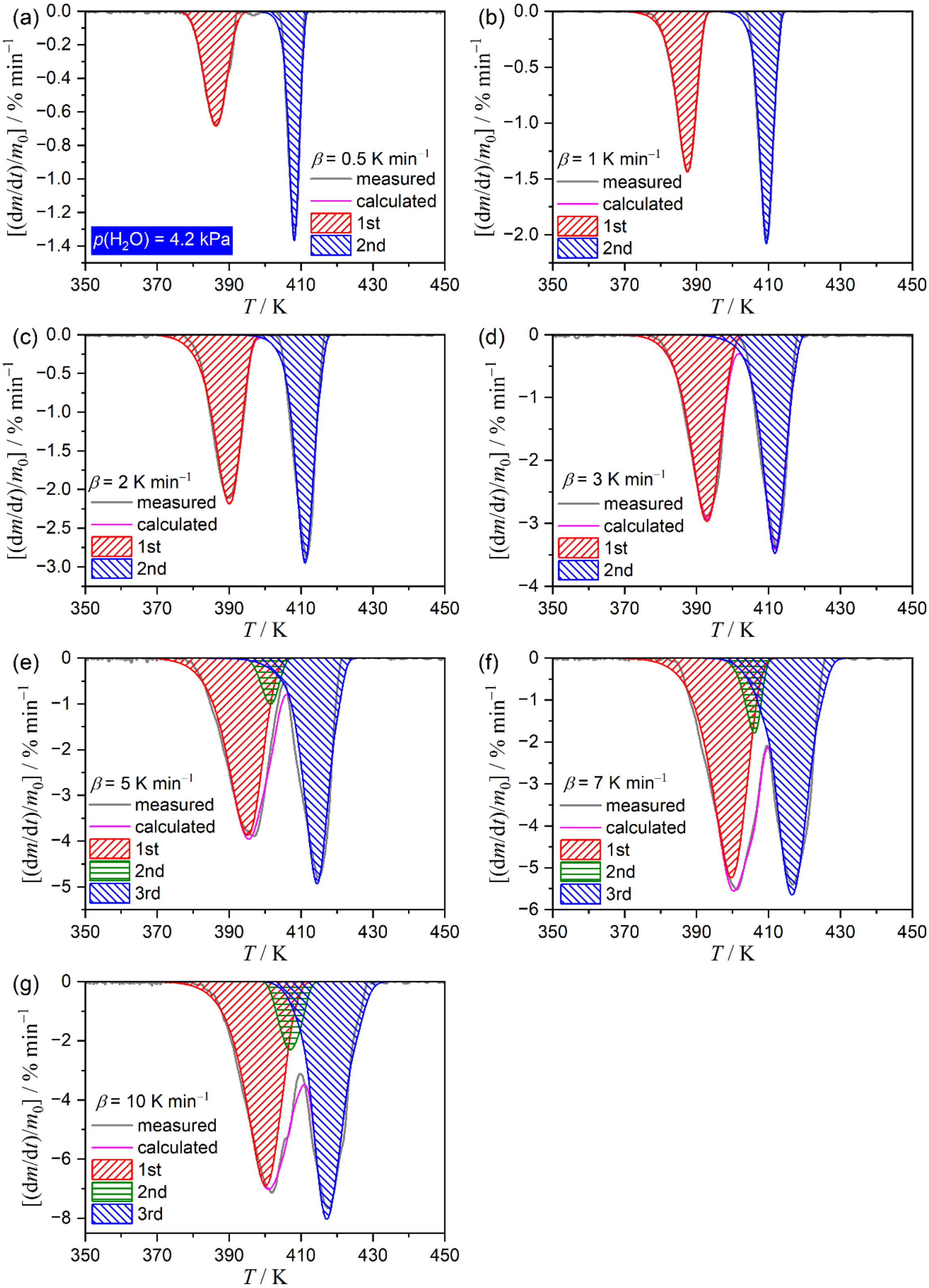

Figure S3. MDA results for the thermal dehydration process of CC-DH (m_0 = 3.03 ± 0.05 mg) to form CC-AH under linear nonisothermal conditions at various β values in a stream of wet N_2 with $p(H_2O)$ = 4.2 kPa.

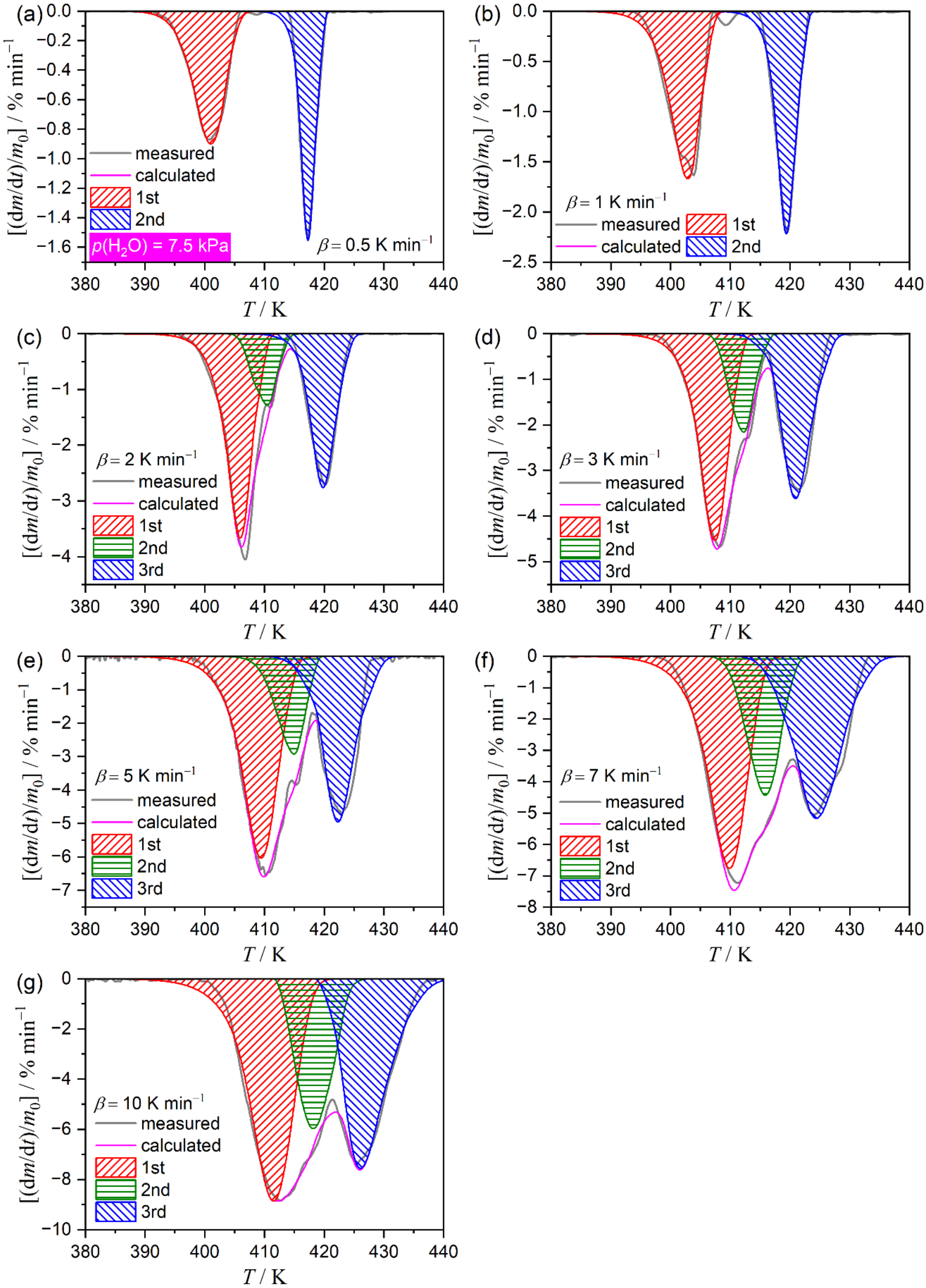

Figure S4. MDA results for the thermal dehydration process of CC-DH (m_0 = 3.02 ± 0.04 mg) to form CC-AH under linear nonisothermal conditions at various β values in a stream of wet N_2 with $p(H_2O)$ = 7.5 kPa.

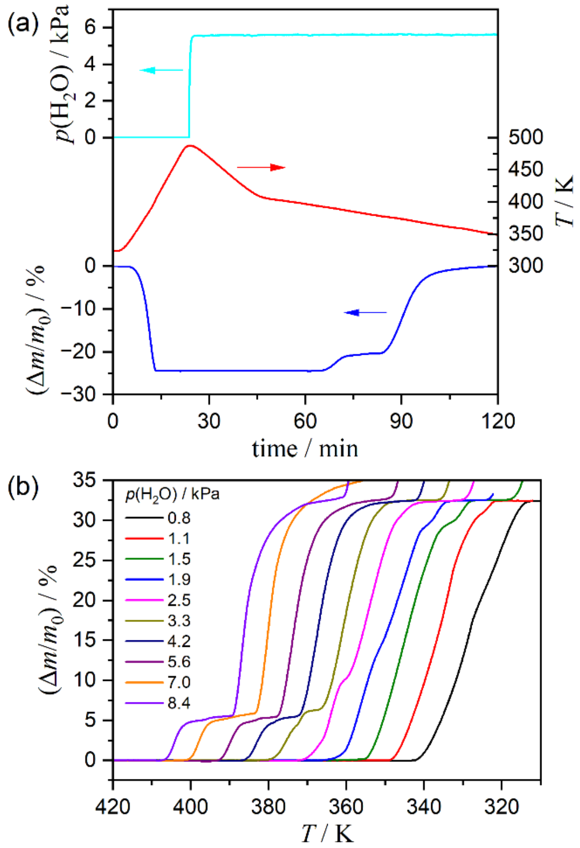

Figure S5. TG curves for hydration process of CC-AH under linear cooling at 1 K min^{-1} in a stream of wet N_2 (q_v = 200 cm^3 min^{-1}): (a) typical measurement scheme for the rehydration process and (b) TG curves at various $p(H_2O)$ values. Measurements were performed using a humidity-controlled TG system constructed by coupling TG–DTA (TG8122, Rigaku) and a humidity controller (me-40DP-2PHW, Micro Equipment Co.). Initially, the CC-DH sample (300–500 µm, m_0: approximately 3.0 mg) was heated to 473 K at a β of 5 K min^{-1} in a stream of dry N_2 and subsequently cooled to a temperature of 423–408 K at a cooling rate of 5 K min^{-1}.

S2. Kinetics of the component reaction steps at different $p(H_2O)$ values

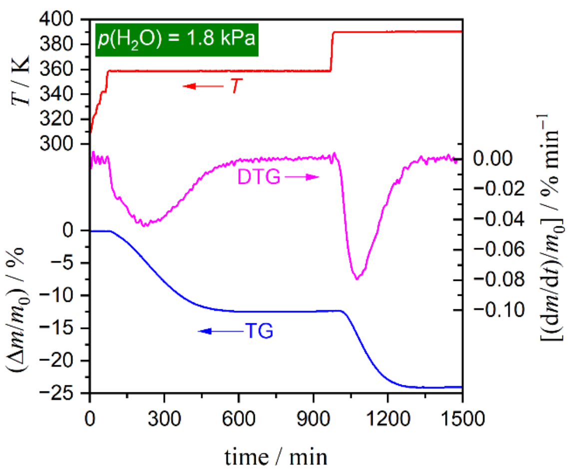

Figure S6. An example of TG–DTG measurement conducted for the two-step thermal dehydration process of CC-DH to form CC-AH via CC-MH recorded by heating the sample (m_0 = 3.084 mg) according to two-step isothermal heating program in a stream of wet N_2 with $p(H_2O)$ = 1.8 kPa.

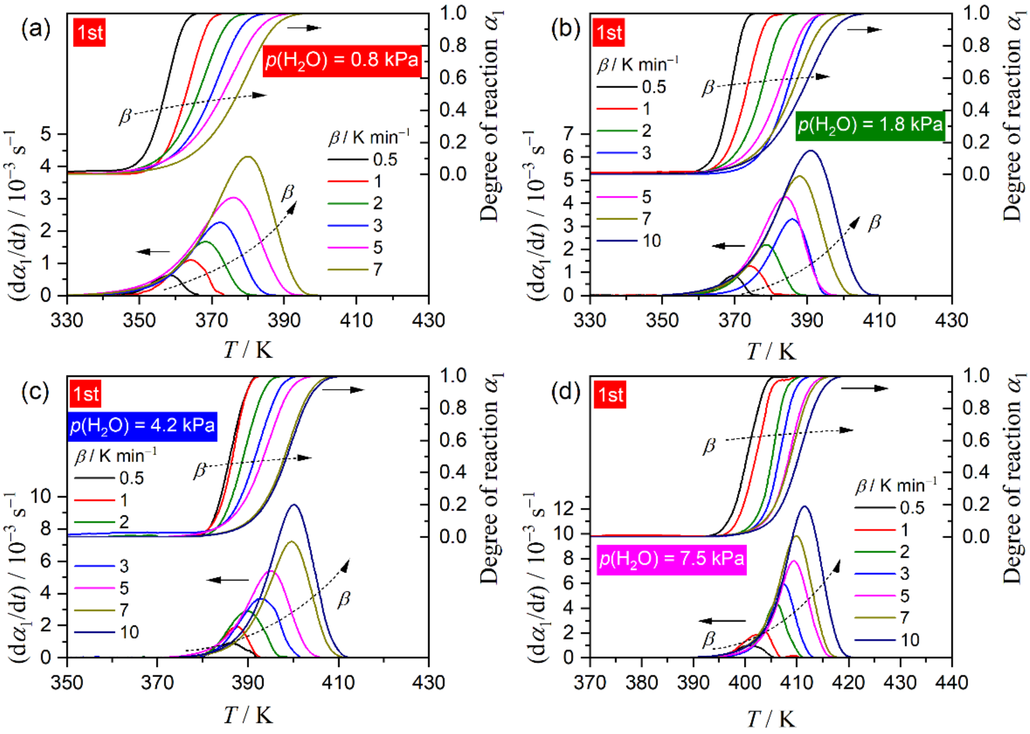

Figure S7. Kinetic curves for the first reaction step of the two-step thermal dehydration of CC-DH to form CC-AH via CC-MH (thermal dehydration of CC-DH to form CC-MH) under linear nonisothermal conditions at various β values in a stream of wet N_2 with different $p(H_2O)$ values, extracted from the overall two-step thermal dehydration process of CC-DH to form CC-AH via CC-MH using MDA: (a) 0.8, (b) 1.8, (c) 4.2, and (d) 7.5 kPa.

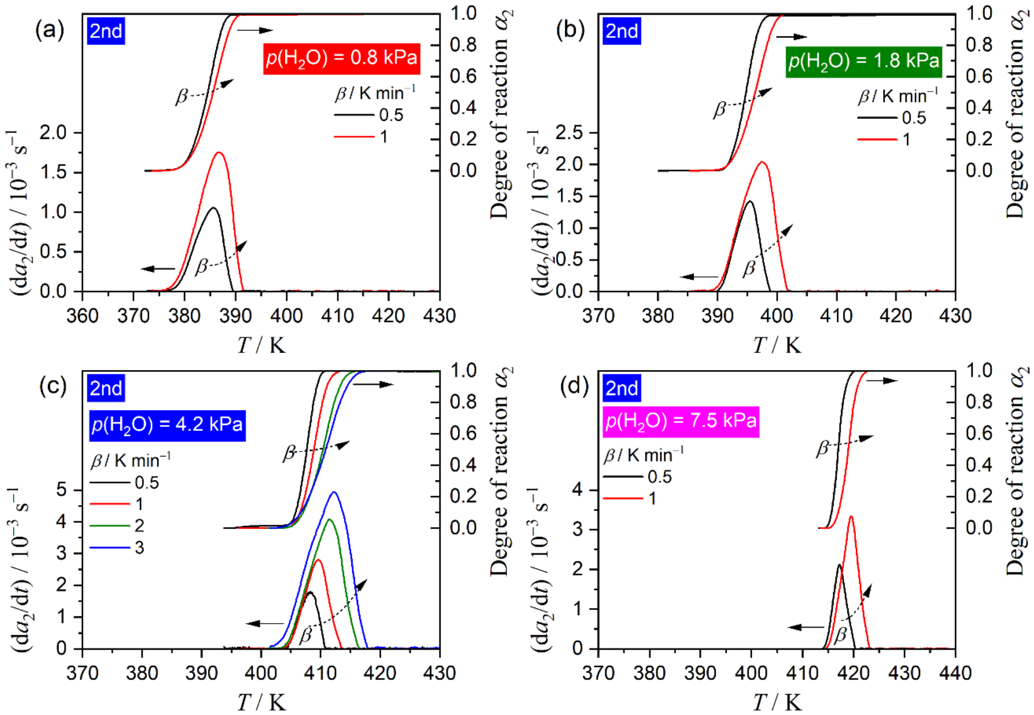

Figure S8. Kinetic curves for the second reaction step of the two-step thermal dehydration of CC-DH to form CC-AH via CC-MH (thermal dehydration of CC-MH to form CC-AH) under linear nonisothermal conditions at different β values in a stream of wet N_2 with different $p(H_2O)$ values, extracted from the overall two-step thermal dehydration process of CC-DH to form CC-AH via CC-MH using MDA: (a) 0.8, (b) 1.8, (c) 4.2, and (d) 7.5 kPa.

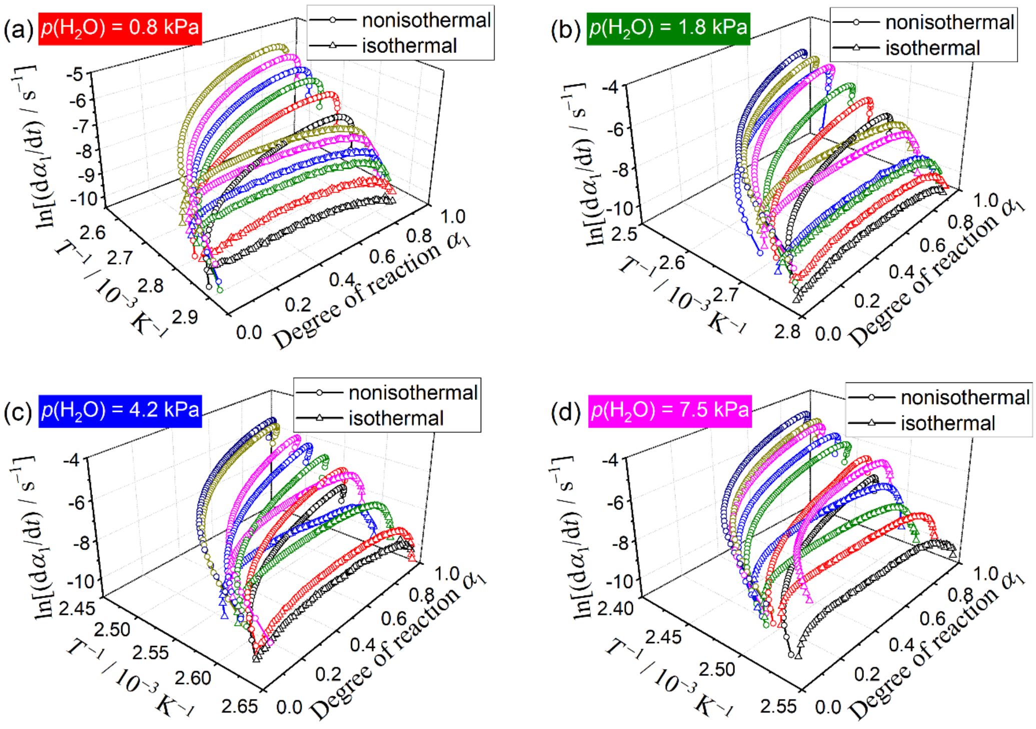

Figure S9. Kinetic curves for the first reaction step of the two-step thermal dehydration process of CC-DH to form CC-AH via CC-MH (thermal dehydration of CC-DH to form CC-MH) under isothermal and linear nonisothermal conditions at various $p(H_2O)$ values, represented in the 3D kinetic coordinate of T^{-1}, α_1, and $\ln(d\alpha_1/dt)$: (a) 0.8, (b) 1.8, (c) 4.2, and (d) 7.5 kPa.

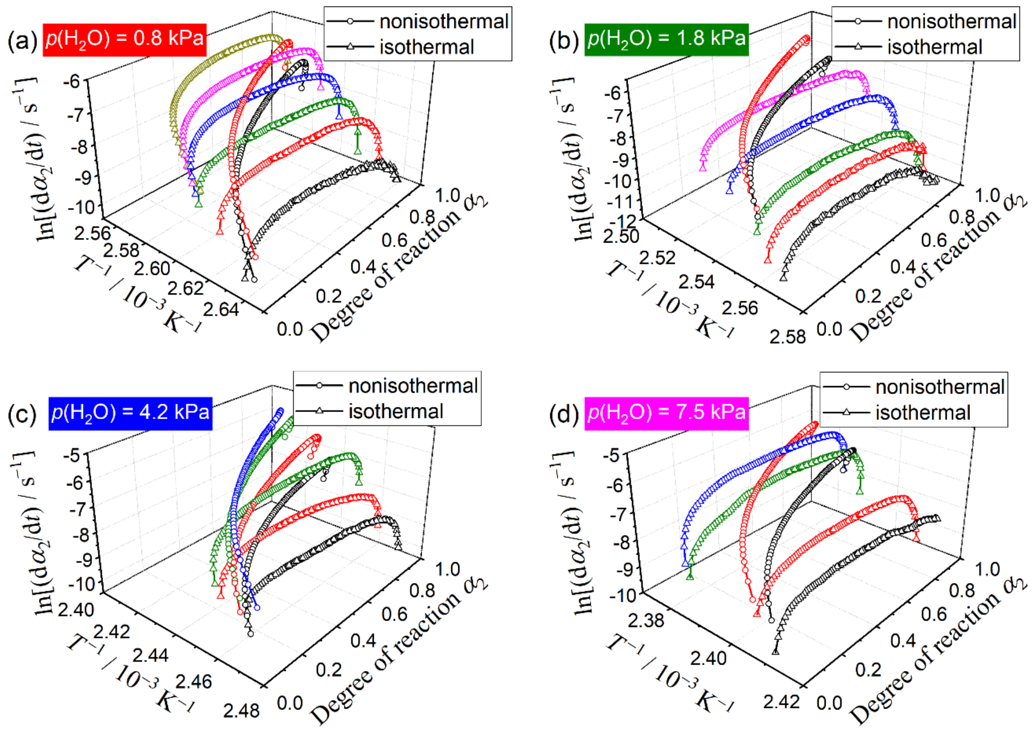

Figure S10. Kinetic curves for the second reaction step of the two-step thermal dehydration process of CC-DH to form CC-AH via CC-MH (thermal dehydration of CC-MH to form CC-AH) under isothermal and linear nonisothermal conditions at various $p(H_2O)$ values, represented in the 3D kinetic coordinate of T^{-1}, α_2, and $\ln(d\alpha_2/dt)$: (a) 0.8, (b) 1.8, (c) 4.2, and (d) 7.5 kPa.

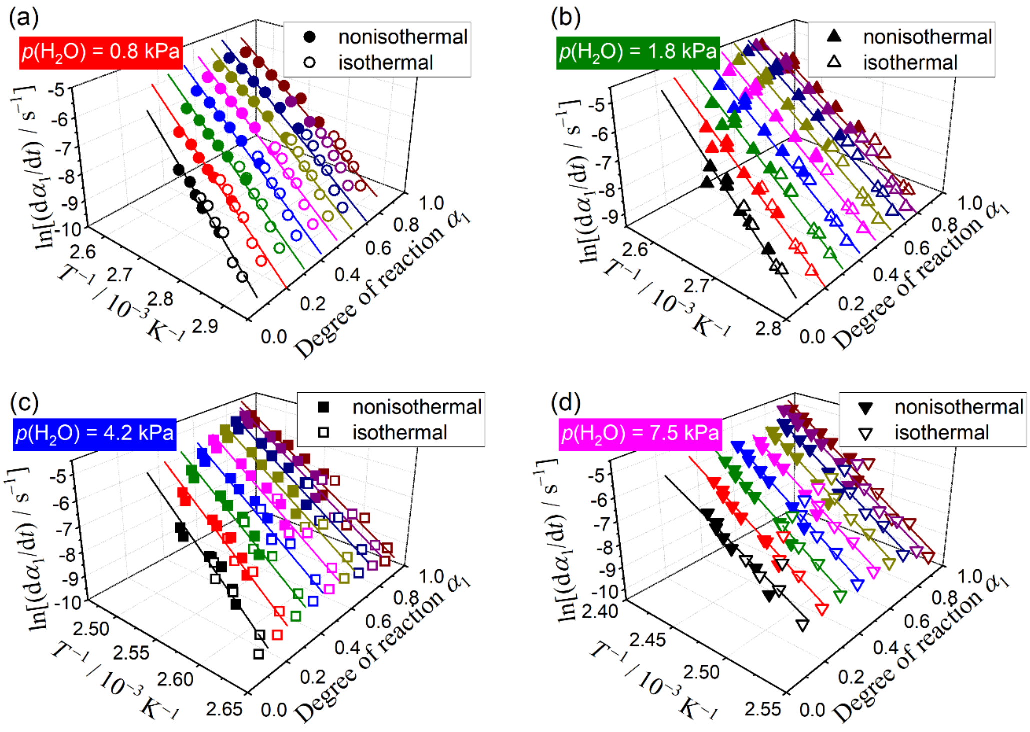

Figure S11. Friedman plots at different α_1 for the first reaction step of the two-step thermal dehydration process of CC-DH to form CC-AH via CC-MH (thermal dehydration of CC-DH to form CC-MH) at various $p(H_2O)$ values: (a) 0.8, (b) 1.8, (c) 4.2, and (d) 7.5 kPa.

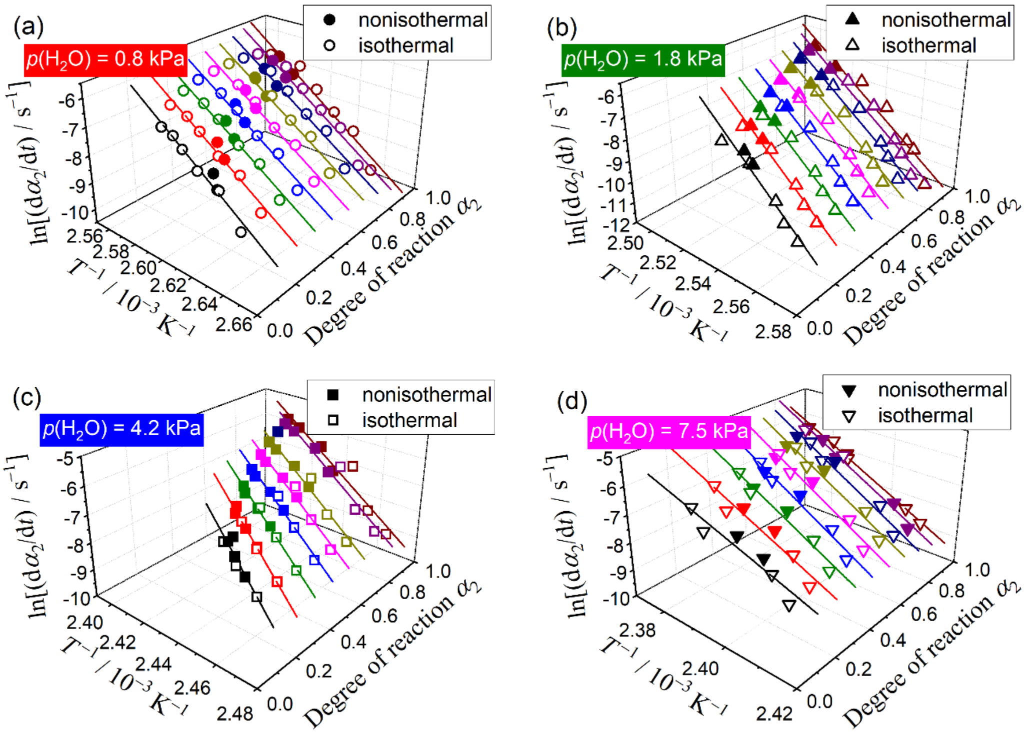

Figure S12. Friedman plots at different α_2 for the second reaction step of the two-step thermal dehydration of CC-DH to form CC-AH via CC-MH (thermal dehydration of CC-MH to form CC-AH) at various $p(H_2O)$ values: (a) 0.8, (b) 1.8, (c) 4.2, and (d) 7.5 kPa.

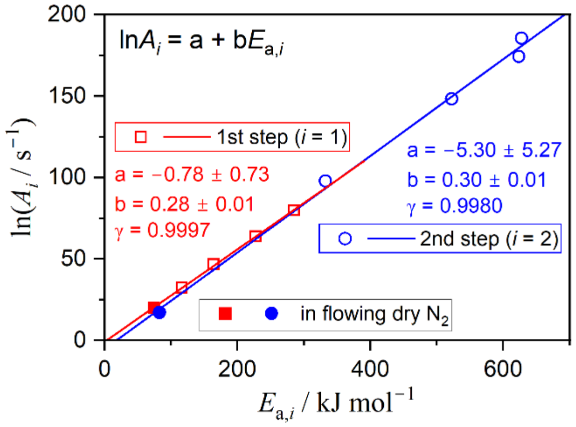

Figure S13. Apparent linear correlations observed between $\ln A_i$ and $E_{a,i}$ values established for the first and second reaction steps of the thermal dehydration process of CC-DH to form CC-AH via CC-MH using the conventional Friedman plot and master plot methods.

S3. Kinetic modeling based on IP–SR–PBR(n) models

Table S1. Differential kinetic equations of IP–SR–PBR(n) models

n	$\frac{\mathrm{d}\alpha}{\mathrm{d}t}$ =
1	a) $t - 1/k_{\mathrm{IP}} \le 1/k_{\mathrm{PBR(1)}}$: $$k_{\mathrm{PBR(1)}}\left[1-\exp\left(-k_{\mathrm{SR}}\left(t-\frac{1}{k_{\mathrm{IP}}}\right)\right)\right]$$
	b) $t - 1/k_{\mathrm{IP}} \ge 1/k_{\mathrm{PBR(1)}}$: $$k_{\mathrm{PBR(1)}}\exp\left(-k_{\mathrm{SR}}\left(t-\frac{1}{k_{\mathrm{IP}}}\right)\right)\left[\exp\left(\frac{k_{\mathrm{SR}}}{k_{\mathrm{PBR(1)}}}\right)-1\right]$$
2	a) $t - 1/k_{\mathrm{IP}} \le 1/k_{\mathrm{PBR(2)}}$: $$-2k_{\mathrm{PBR(2)}}\left[\left(1+\frac{k_{\mathrm{PBR(2)}}}{k_{\mathrm{SR}}}\right)\exp\left(-k_{\mathrm{SR}}\left(t-\frac{1}{k_{\mathrm{IP}}}\right)\right)+k_{\mathrm{PBR(2)}}\left(t-\frac{1}{k_{\mathrm{IP}}}\right)-\left(1+\frac{k_{\mathrm{PBR(2)}}}{k_{\mathrm{SR}}}\right)\right]$$
	b) $t - 1/k_{\mathrm{IP}} \ge 1/k_{\mathrm{PBR(2)}}$: $$-2k_{\mathrm{PBR(2)}}\exp\left(-k_{\mathrm{SR}}\left(t-\frac{1}{k_{\mathrm{IP}}}\right)\right)\left[1+\frac{k_{\mathrm{PBR(2)}}}{k_{\mathrm{SR}}}-\frac{k_{\mathrm{PBR(2)}}}{k_{\mathrm{SR}}}\exp\left(\frac{k_{\mathrm{SR}}}{k_{\mathrm{PBR(2)}}}\right)\right]$$
3	a) $t - 1/k_{\mathrm{IP}} \le 1/k_{\mathrm{PBR(3)}}$: $$-3k_{\mathrm{PBR(3)}}\left[\left(1+2\frac{k_{\mathrm{PBR(3)}}}{k_{\mathrm{SR}}}+2\left(\frac{k_{\mathrm{PBR(3)}}}{k_{\mathrm{SR}}}\right)^2\right)\exp\left(-k_{\mathrm{SR}}\left(t-\frac{1}{k_{\mathrm{IP}}}\right)\right)-\left(-k_{\mathrm{PBR(3)}}\left(t-\frac{1}{k_{\mathrm{IP}}}\right)\right)^2 + 2k_{\mathrm{PBR(3)}}\left(\frac{k_{\mathrm{PBR(3)}}}{k_{\mathrm{SR}}}+1\right)\left(t-\frac{1}{k_{\mathrm{IP}}}\right)-\left(1+2\frac{k_{\mathrm{PBR(3)}}}{k_{\mathrm{SR}}}+2\left(\frac{k_{\mathrm{PBR(3)}}}{k_{\mathrm{SR}}}\right)^2\right)\right]$$
	b) $t - 1/k_{\mathrm{IP}} \ge 1/k_{\mathrm{PBR(3)}}$: $$3k_{\mathrm{PBR(3)}}\exp\left(-k_{\mathrm{SR}}\left(t-\frac{1}{k_{\mathrm{IP}}}\right)\right)\left[2\left(\frac{k_{\mathrm{PBR(3)}}}{k_{\mathrm{SR}}}\right)^2\left(\exp\left(\frac{k_{\mathrm{SR}}}{k_{\mathrm{PBR(3)}}}\right)-1\right)-\left(1+2\frac{k_{\mathrm{PBR(3)}}}{k_{\mathrm{SR}}}\right)\right]$$

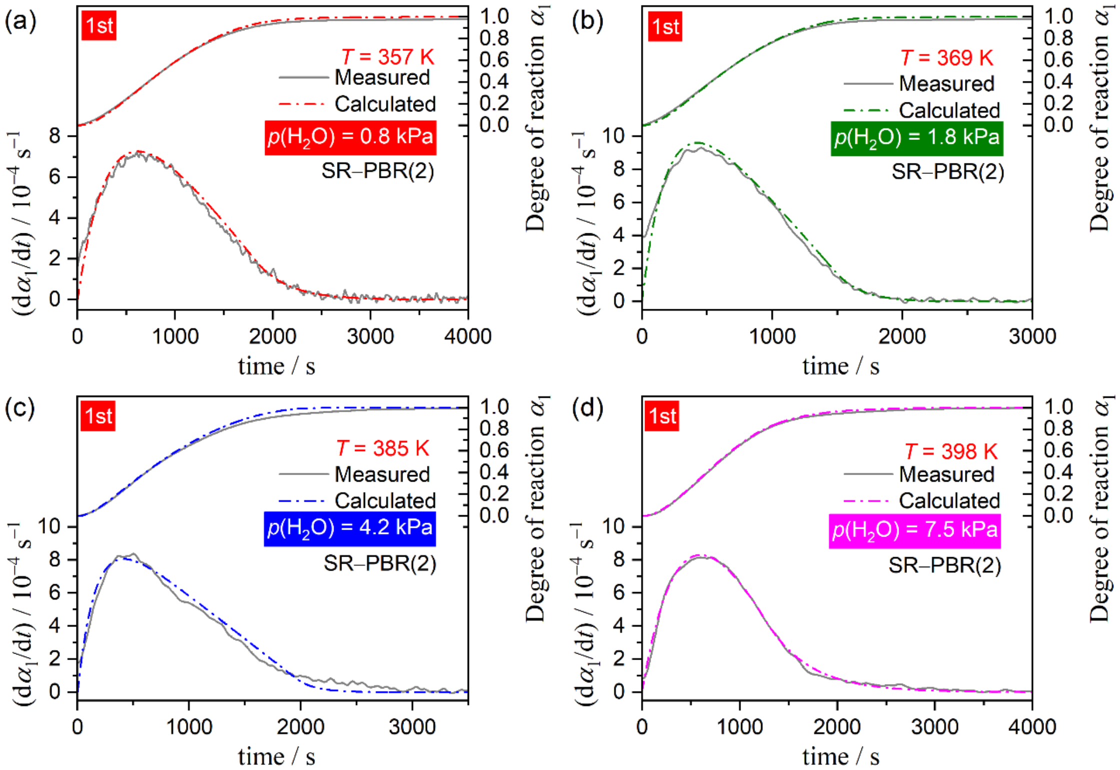

Figure S14. Typical fitting results using SR–PBR(2) model for the first reaction step of the two-step thermal dehydration process of CC-DH to form CC-AH via CC-MH (thermal dehydration of CC-DH to form CC-MH) under isothermal conditions at various $p(H_2O)$ values: (a) 0.8, (b) 1.8, (c) 4.2, and (d) 7.5 kPa.

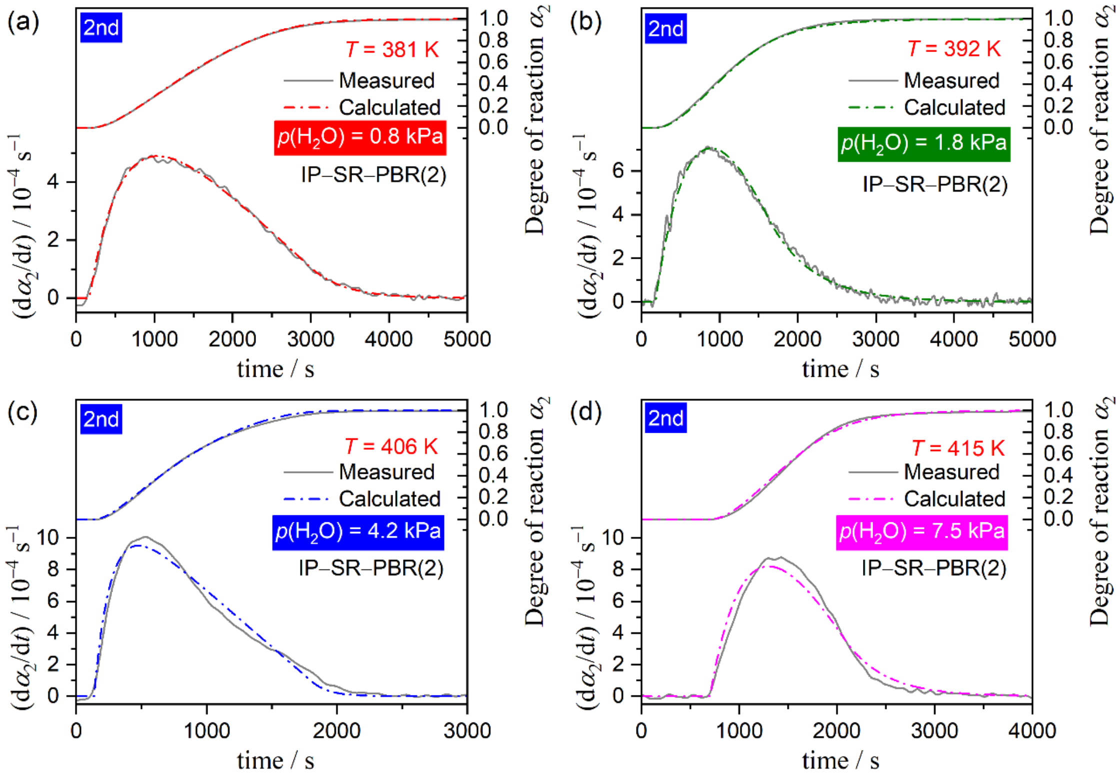

Figure S15. Typical fitting results using IP–SR–PBR(2) model for the second reaction step of the two-step thermal dehydration process of CC-DH to form CC-AH via CC-MH (thermal dehydration of CC-MH to form CC-AH) under isothermal conditions at various $p(H_2O)$ values: (a) 0.8, (b) 1.8, (c) 4.2, and (d) 7.5 kPa.

Table S2. Optimized rate constants of the SR–PBR(n) models for the first reaction step of the two-step thermal dehydration process of CC-DH to form CC-AH via CC-MH (thermal dehydration of CC-DH to form CC-MH) at various temperatures and $p(H_2O)$ values

model	$p(H_2O)$/kPa	T/K	Rate constant			$R^{2,a}$
			$k_{IP,1}/s^{-1}$	$k_{SR,1}/s^{-1}$	$k_{PBR(n),1}/s^{-1}$	
SR–PBR(3)	0.8	356.7	------	3.75×10^{-3}	3.67×10^{-4}	0.9922
		354.6	------	3.05×10^{-3}	2.90×10^{-4}	0.9948
		352.5	------	1.86×10^{-3}	1.82×10^{-4}	0.9946
		350.3	------	1.51×10^{-3}	1.30×10^{-4}	0.9848
		347.8	------	9.65×10^{-4}	6.24×10^{-5}	0.9822
		345.3	------	7.39×10^{-4}	3.70×10^{-5}	0.9789
	1.7	368.8	------	3.62×10^{-3}	5.68×10^{-4}	0.9965
		366.5	------	1.74×10^{-3}	4.02×10^{-4}	0.9910
		362.4	------	6.02×10^{-4}	1.50×10^{-4}	0.9741
		361.4	------	5.88×10^{-4}	1.41×10^{-4}	0.9903
		359.4	------	3.68×10^{-4}	7.12×10^{-5}	0.9726
	4.1	387.8	------	5.83×10^{-3}	1.48×10^{-3}	0.9353
		382.4	------	2.22×10^{-3}	5.65×10^{-4}	0.9690
		378.5	------	7.26×10^{-4}	1.91×10^{-4}	0.9211
	7.4	402.3	------	8.44×10^{-3}	2.05×10^{-3}	0.9427
		400.3	------	4.07×10^{-3}	1.00×10^{-3}	0.9860
		398.0	------	2.19×10^{-3}	5.94×10^{-4}	0.9960
		395.5	------	2.21×10^{-3}	3.57×10^{-4}	0.9955
		392.7	------	7.54×10^{-4}	1.51×10^{-4}	0.9957
SR–PBR(2)	0.8	356.7	------	4.55×10^{-3}	4.98×10^{-4}	0.9921
		354.6	------	4.32×10^{-3}	3.63×10^{-4}	0.9963
		352.5	------	2.61×10^{-3}	2.28×10^{-4}	0.9964
		350.3	------	2.34×10^{-3}	1.74×10^{-4}	0.9941
		347.8	------	1.61×10^{-3}	8.00×10^{-5}	0.9753
		345.3	------	1.23×10^{-3}	4.77×10^{-5}	0.9876
	1.7	368.8	------	3.59×10^{-3}	7.72×10^{-4}	0.9944
		366.5	------	1.99×10^{-3}	5.01×10^{-4}	0.9975
		362.4	------	6.65×10^{-4}	1.91×10^{-4}	0.9864
		361.4	------	7.18×10^{-4}	1.70×10^{-4}	0.9943
		359.4	------	3.30×10^{-4}	1.03×10^{-4}	0.9867
	4.1	387.8	------	6.82×10^{-3}	1.83×10^{-3}	0.9869
		382.4	------	2.39×10^{-3}	7.32×10^{-4}	0.9831
		378.5	------	7.80×10^{-4}	2.51×10^{-4}	0.9423
	7.4	402.3	------	9.93×10^{-3}	2.64×10^{-3}	0.9632
		400.3	------	5.43×10^{-3}	1.17×10^{-3}	0.9930
		398.0	------	3.26×10^{-3}	7.84×10^{-4}	0.9711
		395.5	------	2.53×10^{-3}	4.55×10^{-4}	0.9964
		392.7	------	1.00×10^{-3}	1.78×10^{-4}	0.9959

[a] Determination coefficient of the nonlinear least-squares analysis.

Table S3. Optimized rate constants of the IP–SR–PBR(n) models for the second reaction step of the two-step thermal dehydration process of CC-DH to form CC-AH via CC-MH (thermal dehydration of CC-MH to form CC-AH) at various temperatures and $p(H_2O)$ values

model	$p(H_2O)$/kPa	T/K	Rate constant			$R^{2, a}$
			$k_{IP,2}/s^{-1}$	$k_{SR,2}/s^{-1}$	$k_{PBR(n),2}/s^{-1}$	
IP–SR–PBR(3)	0.8	386.7	------	6.30×10^{-3}	1.29×10^{-3}	0.9792
		384.7	------	3.89×10^{-3}	8.37×10^{-4}	0.9948
		382.8	9.43×10^{-3}	2.38×10^{-3}	4.30×10^{-4}	0.9942
		380.8	5.00×10^{-3}	1.47×10^{-3}	3.05×10^{-4}	0.9916
		378.9	2.75×10^{-3}	8.09×10^{-4}	9.88×10^{-5}	0.9961
	1.7	394.8	1.06×10^{-2}	3.25×10^{-3}	7.43×10^{-4}	0.9903
		392.4	5.00×10^{-3}	2.19×10^{-3}	4.57×10^{-4}	0.9989
		390.6	1.25×10^{-3}	8.93×10^{-4}	1.04×10^{-4}	0.9476
		390.0	7.89×10^{-4}	6.49×10^{-4}	6.37×10^{-5}	0.9250
	4.2	408.2	1.69×10^{-2}	9.19×10^{-3}	1.55×10^{-3}	0.9686
		406.5	7.35×10^{-3}	3.59×10^{-3}	5.85×10^{-4}	0.9941
		404.5	2.85×10^{-3}	1.75×10^{-3}	2.52×10^{-4}	0.9746
		402.7	7.98×10^{-4}	------	------	------
	7.5	419.6	1.11×10^{-2}	9.78×10^{-3}	1.79×10^{-3}	0.9462
		415.3	1.43×10^{-3}	2.26×10^{-3}	5.69×10^{-4}	0.9779
		413.5	9.09×10^{-4}	8.02×10^{-4}	2.76×10^{-4}	0.9811
IP–SR–PBR(2)	0.8	386.7	------	7.68×10^{-3}	1.60×10^{-3}	0.9872
		384.7	------	5.07×10^{-3}	9.84×10^{-4}	0.9989
		382.8	9.43×10^{-3}	3.35×10^{-3}	5.00×10^{-4}	0.9984
		380.8	5.95×10^{-3}	2.32×10^{-3}	3.54×10^{-4}	0.9993
		378.9	2.75×10^{-3}	1.12×10^{-3}	1.16×10^{-4}	0.9940
	1.7	394.8	1.14×10^{-2}	4.53×10^{-3}	8.91×10^{-4}	0.9935
		392.4	5.00×10^{-3}	1.78×10^{-3}	7.04×10^{-4}	0.9959
		390.6	1.25×10^{-3}	1.27×10^{-3}	1.48×10^{-4}	0.9734
		390.0	7.89×10^{-4}	6.49×10^{-4}	6.82×10^{-5}	0.9806
	4.2	408.2	1.69×10^{-2}	7.76×10^{-3}	1.89×10^{-3}	0.9872
		406.5	7.35×10^{-3}	3.77×10^{-3}	7.72×10^{-4}	0.9819
		404.5	3.40×10^{-3}	1.75×10^{-3}	3.67×10^{-4}	0.9799
		402.7	7.98×10^{-4}	------	------	------
	7.5	419.6	1.11×10^{-2}	9.79×10^{-3}	3.23×10^{-3}	0.9823
		415.3	1.43×10^{-3}	2.47×10^{-3}	7.30×10^{-4}	0.9895
		413.5	9.09×10^{-4}	9.95×10^{-4}	3.38×10^{-4}	0.9851

[a] Determination coefficient of the nonlinear least-squares analysis.

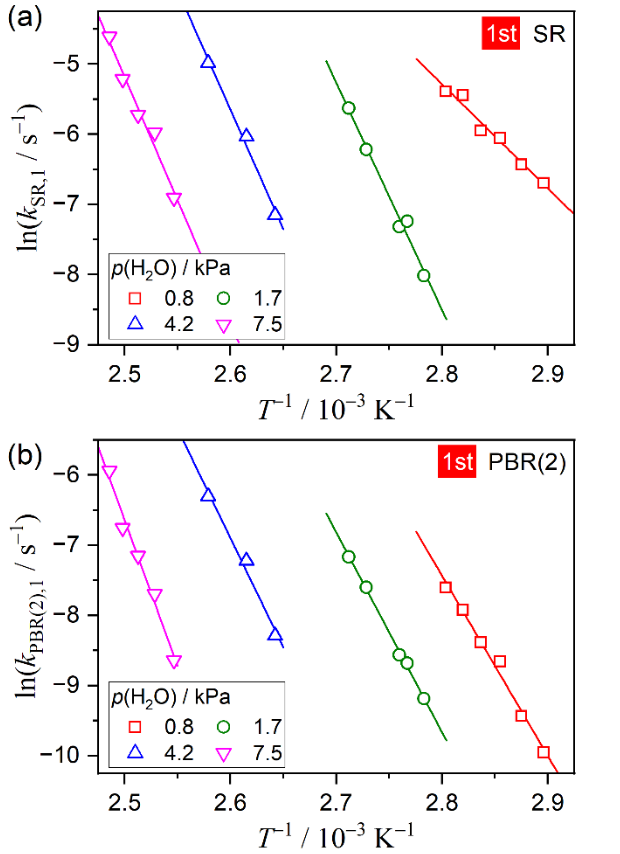

Figure S16. Arrhenius plots of the individual physico-geometrical reaction steps for the first reaction step of the two-step thermal dehydration process of CC-DH to form CC-AH via CC-MH (thermal dehydration of CC-DH to form CC-MH) at varying $p(H_2O)$ values: (a) SR and (b) PBR(2).

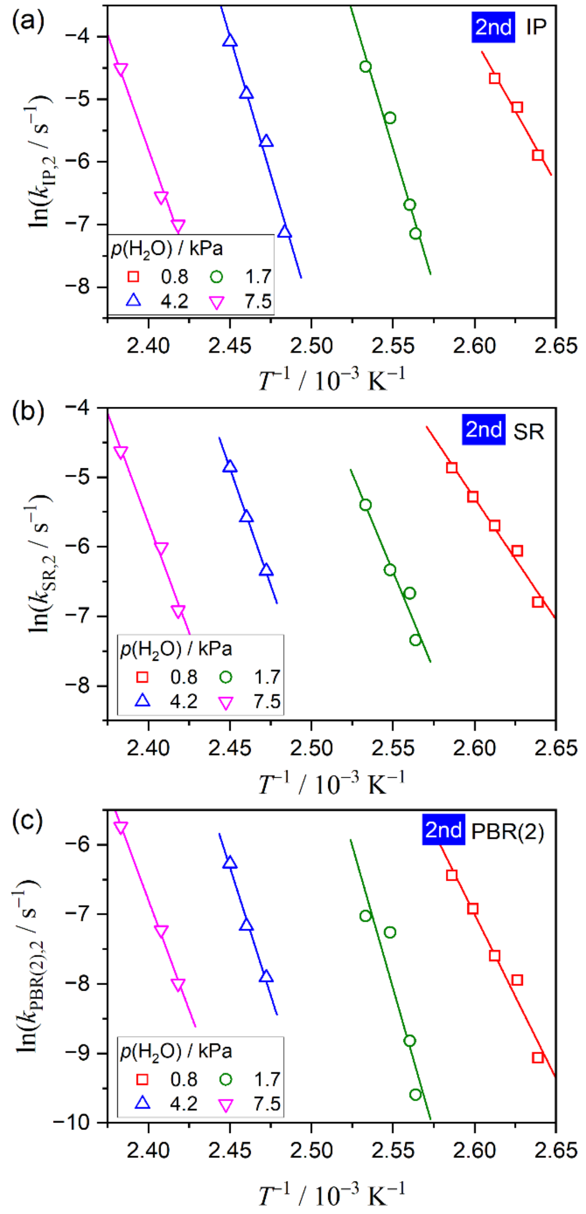

Figure S17. Arrhenius plots of the individual physico-geometrical reaction steps for the second reaction step of the two-step thermal dehydration process of CC-DH to form CC-AH via CC-MH (thermal dehydration of CC-MH to form CC-AH) at varying $p(H_2O)$ values: (a) IP, (b) SR, and (c) PBR(2).

Table S4. Apparent Arrhenius parameters of the component physico-geometrical processes involved in the two-step thermal dehydration process of CC-DH to form CC-AH via CC-MH at different $p(H_2O)$ values, as determined based on the SR–PBR(2) and IP–SR–PBR(2) models

Reaction step i	Process	$p(H_2O)$/kPa	$E_{a,i}$/kJ mol^{-1}	ln(A_i/s^{-1})	$-\gamma$ [a]
1	SR	0.8	123.4 ± 10.5	36.3 ± 3.6	0.9858
		1.7	269.3 ± 20.1	82.2 ± 6.6	0.9918
		4.1	283.2 ± 28.9	82.9 ± 9.1	0.9948
		7.4	291.7 ± 26.9	82.5 ± 8.1	0.9875
	PBR(2)	0.8	213.6 ± 12.2	64.5 ± 4.2	0.9935
		1.7	236.8 ± 5.9	70.1 ± 1.9	0.9991
		4.1	258.9 ± 33.4	74.1 ± 10.5	0.9918
		7.4	345.2 ± 25.9	97.1 ± 7.8	0.9916
2	IP	0.8	384.9 ± 64.6	116.3 ± 20.4	0.9862
		1.7	724.9 ± 96.4	216.5 ± 29.6	0.9828
		4.2	733.3 ± 152.4	227.0 ± 45.3	0.9890
		7.5	607.9 ± 73.2	169.7 ± 21.2	0.9928
	SR	0.8	290.6 ± 24.1	85.6 ± 7.6	0.9898
		1.7	469.3 ± 84.9	137.6 ± 26.1	0.9688
		4.2	558.4 ± 19.7	159.7 ± 5.8	0.9994
		7.5	525.0 ± 60.7	145.9 ± 17.5	0.9934
	PBR(2)	0.8	393.3 ± 43.4	116.0 ± 13.6	0.9822
		1.7	681.3 ± 205.4	200.9 ± 63.0	0.9199
		4.2	611.7 ± 65.2	173.9 ± 19.3	0.9944
		7.5	526.0 ± 27.7	145.1 ± 8.0	0.9986

[a] Correlation coefficient of the linear regression analysis for the Arrhenius plot.

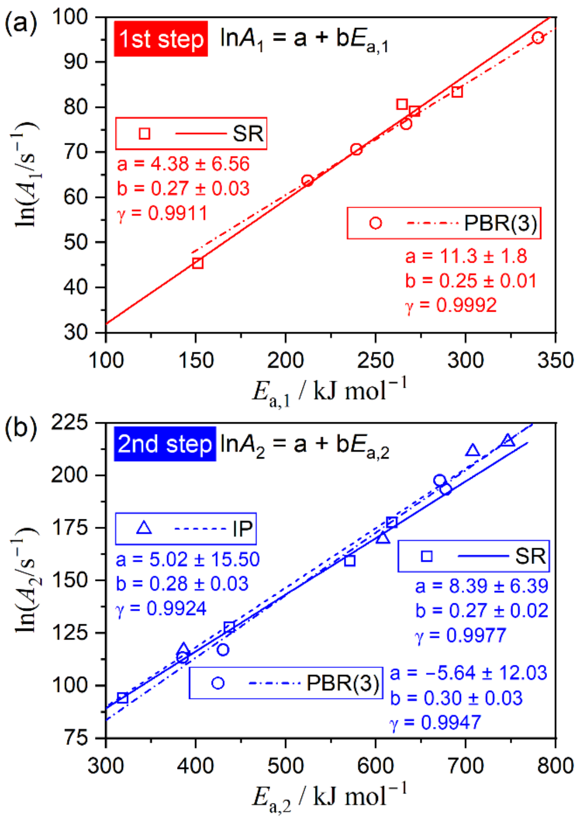

Figure S18. Apparent linear correlations observed between lnA_i and $E_{a,i}$ values determined for the individual physico-geometrical reaction processes of the first and second reaction steps of the thermal dehydration process of CC-DH to form CC-AH via CC-MH based on SR–PBR(3) and IP–SR–PBR(3) models, respectively: (a) first and (b) second reaction steps.